Hindawi Publishing Corporation
International Journal of Polymer Science
Volume 2013, Article ID 905471, 10 pages
http://dx.doi.org/10.1155/2013/905471

Research Article

Rapid Synthesis of Superabsorbent Smart-Swelling Bacterial Cellulose/Acrylamide-Based Hydrogels for Drug Delivery

Manisha Pandey, Mohd Cairul Iqbal Mohd Amin, Naveed Ahmad, and Muhammad Mustafa Abeer

Centre for Drug Delivery Research, Faculty of Pharmacy, Universiti Kebangsaan Malaysia, Jalan Raja Muda Abdul Aziz, 50300 Kuala Lumpur, Malaysia

Correspondence should be addressed to Mohd Cairul Iqbal Mohd Amin; mciamin@yahoo.co.uk

Received 9 May 2013; Revised 19 July 2013; Accepted 23 July 2013

Academic Editor: Yulin Deng

This study evaluated the effect of solubilized and dispersed bacterial cellulose (BC) on the physicochemical characteristics and drug release profile of hydrogels synthesized using biopolymers. Superabsorbent hydrogels were synthesized by graft polymerization of acrylamide on BC solubilized in an NaOH/urea solvent system and on dispersed BC by using N, N'-methylenebisacrylamide as a crosslinker under microwave irradiation. Fourier transform infrared spectroscopy analysis of the resulting hydrogels confirmed the grafting, and an X-ray diffraction pattern showed a decrease in the crystallinity of BC after the grafting process. The hydrogels exhibited pH and ionic responsive swelling behavior, with hydrogels prepared using solubilized BC (SH) having higher swelling ratios. Furthermore, compared to the hydrogels synthesized using dispersed BC, the hydrogels synthesized using solubilized BC showed higher porosity, drug loading efficiency, and release. These results suggest the superiority of the hydrogels prepared using solubilized BC and that they should be explored further for oral drug delivery.

1. Introduction

Currently, natural polymers are being extensively explored for the fabrication of hydrogels, owing to their biodegradability, biocompatibility, nontoxicity, and availability. Consequently, considerable attention has been given to bacterial cellulose (BC), a natural polymer, because of its high mechanical strength, thermal stability, biocompatibility, and purity [1]. However, its application in the synthesis of hydrogels is limited by its insolubility in common solvents owing to strong inter- and intramolecular hydrogen bonding. Thus, solubilization of BC in appropriate solvents could extend its application in the fabrication of films, hydrogels, and membranes and improve its purity and mechanical strength for pharmaceutical and biomedical applications. Although this macromolecule has been successfully solubilized in lithium chloride/*N,N*-dimethylacetamide [2] and *N*-methylmorpholine-*N*-oxide monohydrate [3], its use is limited to laboratory-scale operation because it is highly toxic. To overcome this challenge, a sodium hydroxide (NaOH) complex solvent was prepared. Cellulose with a low degree of polymerization (DP < 300) has been reported to easily dissolve in NaOH (7–10% w/v) at low temperatures (−5°C to −15°C) [4]. Conversely, cellulose with a high degree of polymerization (DP > 300) has been found not to be easily dissolve in NaOH solution alone [5]. The degree of polymerization of BC is in the range of 2000 and 6000 [6], but in some cases it reaches even 16,000 to 20,000 [7]. So, a combination of urea and thiourea with NaOH has been shown to improve the dissolution of BC [8].

The applications of BC in hydrogel synthesis have been limited by its low absorptive ability due to the formation of strong intra- and interhydrogen bonds after drying. However, formation of a double-network structure by combining BC with other polymers (gelatin and chitosan) [9, 10] or graft copolymerization [11–14] has been shown to overcome the problem. Graft copolymerization of BC is mainly performed by free radical polymerization [15] and ionizing radiation

[13, 14]. Accelerated microwave irradiation has gained a lot of attention because of the following factors associated with it: safety concerns, low energy consumption, and low production cost [16, 17]. Compared to hydrogels synthesized using water bath method, hydrogels synthesized using microwave irradiation have greater porosity ($0.05–0.15 \times 10^{-2}$ cm^3/g versus $0.45–2.7 \times 10^{-2}$ cm^3/g) [18]. Furthermore, Kumar et al. reported that the percentage of grafting of xanthan gum with polyacrylamide (PAM) increased from 12.76% to 87.15% with an increase in irradiation power from 40 W to 100 W, consequentially increasing the drug release rate with an increase in grafting percentage. They also observed a higher drug release rate from the grafted copolymer matrix as compared to the xanthan gum matrix [19].

Over the last two decades, "smart-swelling hydrogels" that exhibit remarkable changes in their swelling behavior in response to environmental stimuli, such as temperature, pH, and ionic strength, have become popular carriers for controlled drug delivery. PAM, which was used in this study, has been reported to produce nonionic hydrogels. However, in the presence of an alkali, PAM is hydrolyzed and produces anionic hydrogels that exhibit higher pH sensitivity than that of nonionic hydrogels. Electrostatic repulsion between the carboxylic groups of the ionic hydrogels results in a pH-responsive swelling of the hydrogel; such pH-responsive swelling behavior can assist in the control of drug release [11, 20–23].

In this study, BC/PAM hydrogels were synthesized using BC dispersion and BC dissolved in NaOH/urea solvent system. Hydrogels were developed by using microwave irradiation instead of the conventional heating method to improve the degree of grafting and reduce the time consumption. The resulting hydrogels were characterized using Fourier transform infrared spectroscopy (FT-IR), X-ray diffraction (XRD), and scanning electron microscopy (SEM). The swelling behavior of the hydrogels was then determined at different pH values and ionic strengths. Finally, drug loading and release behavior of the hydrogels were investigated to evaluate the potential for the application of these hydrogels in drug delivery.

2. Experimental

2.1. Materials. Acrylamide (AM), potassium persulfate (KPS), *N,N′*-methylenebisacrylamide (MBA), and theophylline were purchased from Sigma Aldrich, Japan. Urea, sodium hydroxide, and other reagents were of analytical grade and used without further purification. Phosphate buffer solutions at pH 2, 5, 7, and 9 were prepared as described in the British Pharmacopoeia. Nata de coco was used as a source of BC and was procured from a local food company.

2.2. Purification of Nata de Coco. Nata de coco was purified as previously described [1]. Briefly, nata de coco was washed and soaked in distilled water to attain pH (5–7). To achieve a constant weight, the samples were then blended in a wet blender, poured into trays, and then freeze-dried. Using a pulverizer (Pulverisette 14, Frisch, Germany), the BC sheets were micronized to produce a fluffy BC powder.

2.3. Synthesis of Hydrogels. A solvent system consisting of NaOH/urea was used to dissolve the BC. Two different ratios of NaOH (6% & 8% w/v) and urea (4% w/v) were dissolved in distilled water to prepare the solvent system for dissolution. Next, 2.5 g of BC powder was added to 100 mL of solvent with constant stirring and stored at −10°C for 12 h. The frozen solid was then thawed and stirred extensively at 25°C until a transparent solution was attained [24]. To prepare the BC dispersion, purified BC with a particle size in the range 50–100 μm was dispersed in distilled water to produce 2.5% (w/v) dispersion [25].

To synthesize the BC/PAM hydrogels, AM (2.0 g) was added to 20 mL of freshly prepared BC solution followed by the addition of potassium persulfate as an initiator (7% w/w of AM) and MBA (7% w/w of AM) as a crosslinker. Next, the reaction mixtures were irradiated using a microwave irradiator (LG, model MS2388 K, Korea) at 340 W for 30 s to synthesize hydrogels (SH). Similarly, the hydrogels from the dispersed BC were produced using the same concentration of AM, crosslinker, and initiator, with the exception of BC dispersion being used instead of a solution (DH). Similarly, PAM was prepared by exposure to microwave radiations in the absence of BC as shown in Table 1.

2.4. Characterization of the Hydrogels

2.4.1. Gel Fraction Determination. The gel fractions (GF) of the hydrogels were determined to estimate the degree of grafting. Freshly prepared hydrogel discs (1.2 cm in diameter) were dried in an oven at 60°C to a constant weight (W_0). The dried hydrogel discs were then soaked in distilled water to remove any unreacted monomers or sol from the hydrogels. The water was changed after 24 h, and the absorbance of the solvent used to soak the hydrogels was determined at 270 nm to detect the unreacted PAM. These extracted hydrogels were then dried again to a constant weight (W_1) at a temperature of 60°C in an oven. The percentage of gel fraction (GF %) was calculated using (1) [13, 14]

$$\text{GF } \% = \frac{W_1}{W_0} \times 100. \quad (1)$$

2.4.2. FT-IR Spectroscopic Analysis. IR spectra of the samples were recorded using Perkin Elmer FT-IR Spectra 2000 at room temperature (25°C). The test specimens were prepared using the KBr disc method and analyzed over the range of 400–4000 cm^{-1}.

2.4.3. X-Ray Diffraction. X-ray diffractograms of the BC and hydrogels were obtained using an X-ray diffractometer (D8-Advance, Bruker AXS) with Cu Kα radiation at 40 kV and 50 mA in a differential angle range of 5–60° 2θ [4].

2.4.4. Morphological Analysis. The morphology of the freeze-dried swollen hydrogels was examined using scanning-electron microscopy (Leo 1450 VP, Germany). The freeze-dried samples were mounted on to an aluminum stub with double-sided carbon tape and coated with gold in a sputter coater (SC500; BioRad, UK) under argon atmosphere.

Table 1: Formulation code, gel fraction, and release kinetics of hydrogel.

Code	BC/AM ratio (% w/v)	NaOH/urea ratio (% w/v)	Gel fraction (%) (mean ± SD)	Zero order (g/hr)		First order (hr^{-1})		Peppas	
				R^2	K	R^2	K	R^2	n
PAM	0/10	0/0	87.98 ± 2.42	0.996	0.100	0.844	0.002	0.957	0.794
DH	2.5/10	0/0	82.09 ± 2.1	0.996	0.111	0.841	0.002	0.954	0.775
$SH_{6:4}$	2.5/10	6/4	73.29 ± 1.65	0.991	0.135	0.824	0.002	0.932	0.723
$SH_{8:4}$	2.5/10	8/4	69.5 ± 3.05	0.990	0.149	0.813	0.002	0.921	0.712

2.4.5. Mechanical Properties. The mechanical properties of the hydrogels of similar dimensions (1.2 cm in diameter) were determined using Instron 5567 Universal Testing System equipped with a load cell. The maximum force load was set to 250 N, and the compression rate was 5 mm/min. Strain was determined by measuring the peak of the curve, while the compressive modulus was calculated by measuring the slope of the stress and strain curves. The tests were repeated at least 3 times [26].

2.5. Swelling Studies. The smart swelling behavior of the hydrogels was investigated in buffer solutions at different pH values (2, 5, 7, and 9) and ionic strengths (0.5 M, 0.1 M, 0.01 M, and 0.001 M NaCl). Dried hydrogel (G_d) with a known weight was immersed in 50 mL of the swelling media. The swollen samples were weighed (G_s) at fixed time intervals, and the excess media were removed by blotting with a piece of filter paper. The percentage of swelling ratio (% SR) of the hydrogel was calculated using (2)

$$\%\ \mathrm{SR} = \frac{(G_s - G_d)}{G_d} \times 100. \quad (2)$$

2.6. Drug Release Studies

2.6.1. Drug Loading. Theophylline was loaded as a model drug into the hydrogels (PAM, DH, $SH_{6:4}$, and $SH_{8:4}$) by using a diffusion partition method. The dried hydrogel discs were immersed in 20 mL of drug solution (10 mg/mL) at pH 7.4 for 24 h. The swollen hydrogel discs were removed from the drug solution, washed with distilled water, and dried at 30°C to a constant weight. The concentration of the drug remaining in the solution was determined by measuring the absorbance at 272 nm by using spectrophotometry (UV-1601; Shimadzu, Japan). The drug loading percentage (DL %) was calculated using (3)

$$\mathrm{DL}\ \% = \frac{W_{dg}}{W_g} \times 100, \quad (3)$$

where W_{dg} is the amount of drug entrapped in the hydrogel and W_g is the weight of the dried hydrogel disc.

2.6.2. In Vitro Drug Release Study. Drug release studies from hydrogels were conducted using a submerging theophylline-loaded hydrogel disc into 100 mL of buffer solution at pH 7.4 for up to 24 h. The dissolution media were maintained at a fixed temperature of 37°C with constant agitation at 50 rpm. Aliquots of 4 mL were withdrawn at specific time intervals, and the fluid stock was continuously replenished with fresh media. The concentration of the drug was then measured using a spectrophotometer at 272 nm.

The drug release data for 8 h was fitted to a zero-order, first-order, and Korsmeyer-Peppas equation to determine the type of release kinetics of theophylline from the hydrogels. The value of the release exponent of the Korsmeyer-Peppas (n) equation was used to describe the release mechanism of the drug from the hydrogel [27].

3. Results and Discussion

3.1. Synthesis of the Hydrogels. The main objective of this work was to investigate the effect of the physical state of the BC and solvents on the properties of hydrogels produced from it after irradiation with microwave energy. The BC/PAM hydrogels were successfully synthesized using the accelerated microwave irradiation method by maintaining the entire synthesis parameters constant except for the physical state of the BC, which was either in a dispersed or solubilized form. After 96 h, no residues from the AM were found in the extraction medium, suggesting that soaking the hydrogels for 4 days was sufficient to extract all the unreacted monomers.

3.2. Reaction Mechanism. The reaction mechanism involved in the synthesis of the hydrogel is shown in Figure 1. In the first step, sulfate ion radicals ($SO_4^{-\bullet}$) were produced from potassium persulfate because of microwave irradiation, which further reacted with water molecules to generate hydroxyl radicals ($OH^\bullet$). Moreover, in DH hydrogels, both $SO_4^{-\bullet}$ and $OH^\bullet$ radicals reacted with AM and BC to produce active sites for the reaction. Activated monomers that polymerized and produced PAM chains were then grafted into the BC at the active sites to produce a grafted BC/PAM. PAM and the grafted polymers were further cross-linked by MBA to produce the hydrogel.

Similarly, in hydrogels that were produced from solubilized BC (SHs), the active sites were generated due to the presence of hydroxyl radicals ($OH^\bullet$) and sulfate ion radicals ($SO_4^{-\bullet}$). The activated monomers were polymerized and grafted into the BC backbone and finally cross-linked by MBA. The only difference in the reaction mechanism of the SH was the partial hydrolysis of AM to sodium acrylate in the presence of NaOH. Therefore, the finally synthesized product could also be designated as BC-g-poly (AM-sodium acrylate) hydrogel, which was anionic in nature because of the presence of the carboxylate anion [11].

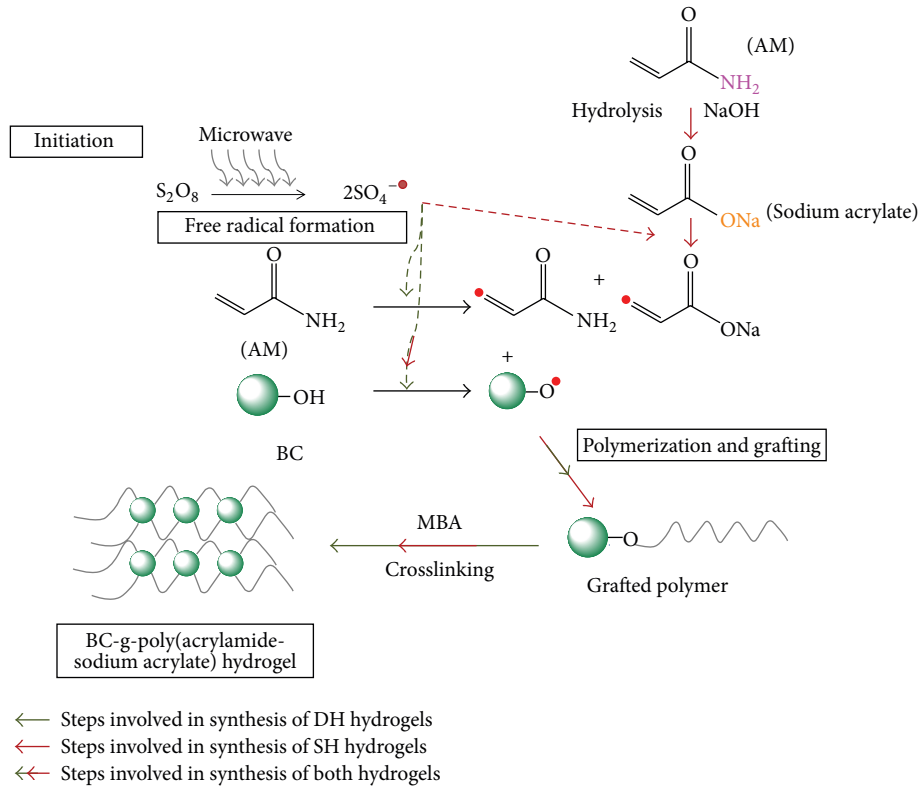

Figure 1: Reaction mechanism of hydrogel synthesis.

3.3. Gel Fractions. The fundamental characteristic of hydrogels is their ability to imbibe and hold a large amount of water while remaining insoluble. The gel fraction of the hydrogels indicates the degree of grafting and cross-linking in the hydrogels. The cross-linking prevents the hydrogels from solubilizing and only enables the expansion of the hydrogel during the extraction; thus, a higher % GF indicates a higher degree of cross-linking. The gel fractions of the hydrogels prepared from solubilized BC ($SH_{6:4}$ and $SH_{8:4}$), dispersed BC (DH), and pure PAM were 73.29±1.65, 69.5±3.05, 82.09± 2.1, and 87.98 ± 2.42, respectively (Table 1). The extracted weights of $SH_{6:4}$ and $SH_{8:4}$ were comparatively lower than those of the DH and PAM hydrogels. This phenomenon could be attributed to NaOH, which may have weakened the cross-linking points, resulting in a decrease in cross-linking density and, consequently, the gel fraction. At higher NaOH concentrations, the polymeric chains were well separated, causing higher sol content. This may also partially be due to weight loss during weighing owing to the fragile nature of the hydrogel at equilibrium swelling. However, the DH and PAM hydrogels exhibited a higher gel fraction percentage throughout the extraction process. Marandi et al. have reported similar observations when pure PAM hydrogels were hydrolyzed using NaOH [20]. However, the gel fraction of the BC/PAM hydrogels containing solubilized BC could be further improved by changing the concentration of the initiator and cross-linker, as well as the microwave irradiation power.

3.4. FT-IR Spectroscopic Analysis. The FT-IR spectra of pure BC, PAM, DH, $SH_{6:4}$, and $SH_{8:4}$ are presented in Figure 2. In the pure BC spectra, peaks at 1059 cm^{-1}, 1163 cm^{-1}, 2914 cm^{-1}, and 3398 cm^{-1} represented C–O stretching vibration, C–O–C stretching of the ether linkage (1,4-β-D-glucoside), C–H stretching and O–H stretching of the intermolecular hydrogen bonds, respectively [14]. However, the PAM spectra exhibited distinct peaks at 3421 and 3215 cm^{-1}, representing N–H asymmetric and symmetric stretching vibrations at 1658 and 1451 cm^{-1}, which corresponded to the C=O stretching of the amide I band and C–N stretching, respectively [28]. The spectra of DH and SH confirmed the presence of PAM with an absorption band at 1655 and 1667 cm^{-1} due to C=O stretching, 1452 cm^{-1} due to C–N stretching, and a broad absorption band at 3438 cm^{-1} due to overlapping O–H stretching of the BC and N–H stretching of AM. The strong absorption band at 2924 and 2929 cm^{-1} can be attributed to an overlap of C–H stretching of the BC and AM in the absence of C–O stretching vibrations at 1059 cm^{-1} in the DH and SH hydrogels spectra, indicating the grafting of PAM onto the BC. The spectra of $SH_{6:4}$ and $SH_{8:4}$ indicated appearance of a new absorbance band at 1568 cm^{-1}, which was assigned to the asymmetric stretching of the carboxylate anion, indicating partial hydrolysis of the amide group into a carboxylate group and production of ammonia. The hydrolysis was further confirmed by the appearance of another sharp peak at 1408 cm^{-1}, which was attributed

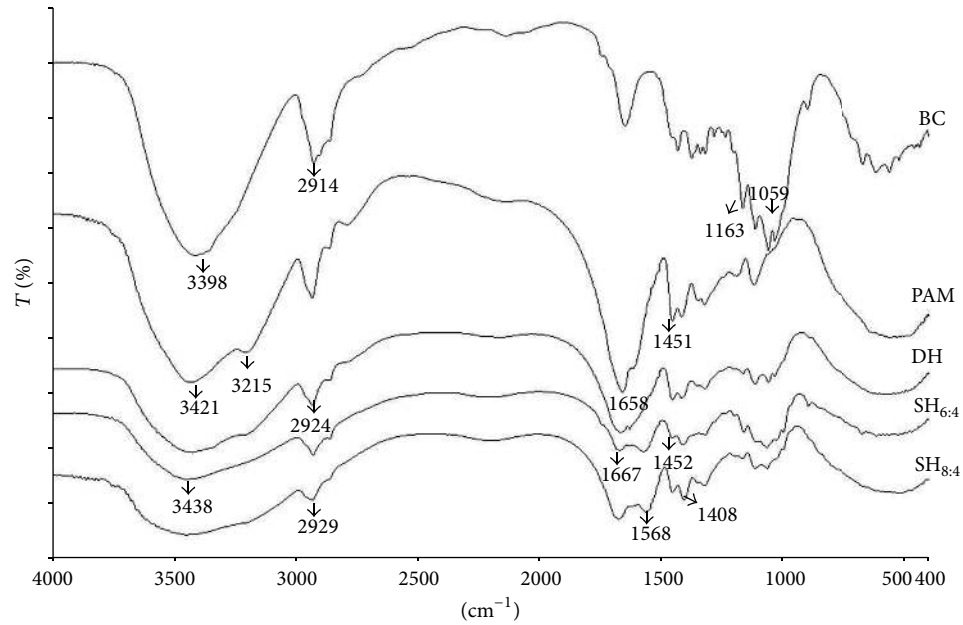

Figure 2: FT-IR spectra of bacterial cellulose (BC), polyacrylamide hydrogel (PAM), and BC/AM hydrogels.

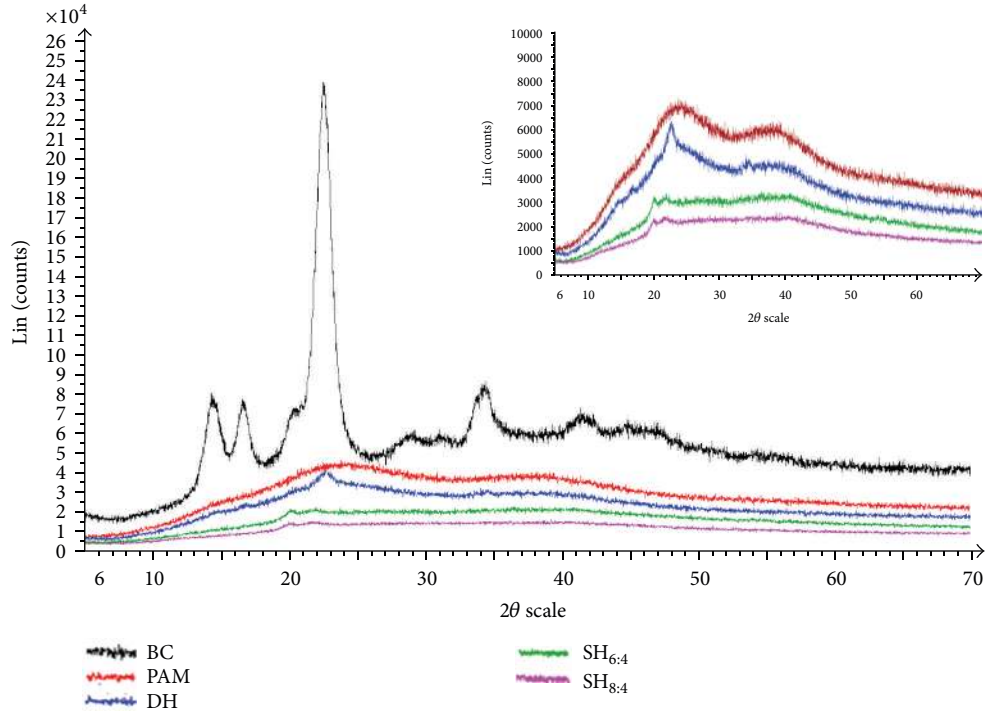

Figure 3: FIGURE 3: X-ray diffractogram of pure bacterial cellulose, polyacrylamide hydrogel, and BC/AM hydrogels.

to the symmetric stretching mode of the carboxylate anion [20, 29].

3.5. X-Ray Diffraction Study. The X-ray diffraction pattern of PAM, DH, $SH_{6:4}$, and $SH_{8:4}$ indicated that the hydrogels exhibited a more amorphous morphology compared to that of pure BC. The diffractogram of pure BC showed a similar pattern with 4 characteristic peaks of cellulose I, located at $2\theta = 14^{\circ}$, 16°, 23°, and 34°, which corresponded to $(1\ 0\ 1)$, $(1\ 0\ \bar{1})$, $(0\ 0\ 2)$, and $(0\ 4\ 0)$ crystallographic plane, respectively [30]. As depicted in Figure 3, the characteristic diffraction at $2\theta = 22.48^{\circ}$ in the DH, 22.02° in $SH_{6:4}$, and $SH_{8:4}$ hydrogels is assigned to the cellulose crystal; however, the peak intensity of the cellulose was reduced in the SH

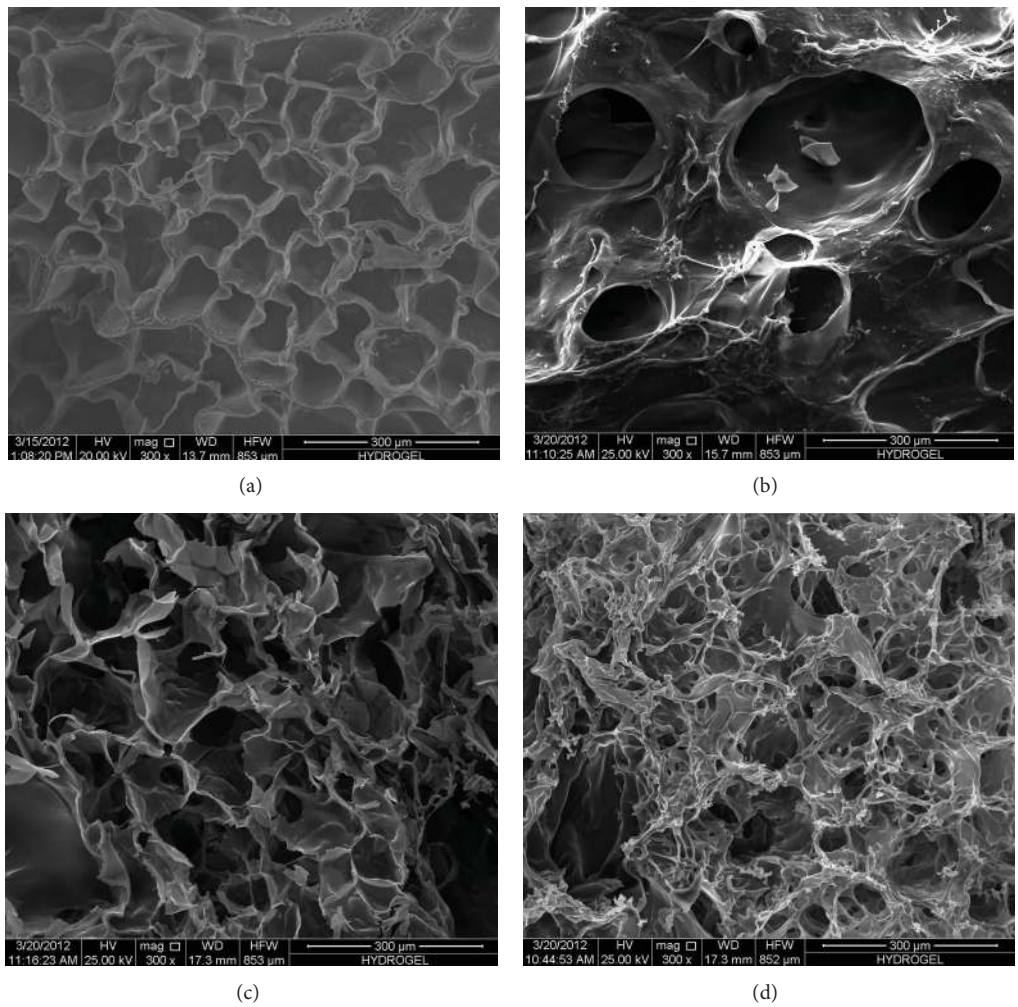

Figure 4: Scanning electron micrograph of (a) PAM, (b) DH, (c) $SH_{6:4}$, and (d) $SH_{8:4}$.

compared to DH, which indicated a more amorphous nature of BC in the SH owing to the alkali treatment. Comparison of the XRD pattern of BC with that of DH revealed decreased crystallinity in the BC when it was grafted with PAM. The disappearance of the characteristic pattern of peaks for cellulose in the DH and SH may be due to the cross-linking between BC and PAM, resulting in the destruction of the initial crystalline arrangement of BC.

3.6. Morphological Analysis. Scanning electron micrographs of the freeze-dried swollen hydrogels are shown in Figure 4. $SH_{6:4}$ and $SH_{8:4}$ exhibited relatively higher porosity than that of DH and PAM. The SEM images of $SH_{6:4}$ and $SH_{8:4}$ demonstrated a well-defined interconnected three-dimensional porous network structure, while the surface pores were much smaller in DH. Interestingly, the surfaces of both SHs were fluffier and exhibited larger and smaller interconnected pores compared to those of DH and PAM. These highly interconnected pores provided more available regions for the diffusion of water molecules, and thus the hydrogel may demonstrate a higher water absorption capacity [14]. The high-porosity structure of the SH was attributed to the electrostatic repulsion resulting from the carboxylate anion ($-COO^-$) group, which was produced as a result of the partial hydrolysis of AM, as previously discussed. NaOH is also responsible for the weakening of the hydrogel by attacking the crosslinking points of polyacrylamide, and as a result the crosslink density decreases. The decrease in crosslink density causes the high swelling capacity of the hydrogel. This observation also supported the proposed reaction mechanism in which the production of ammonia gas during the synthesis process in the presence of NaOH led to the formation of a more porous hydrogel. The amount of ammonia gas liberated was proportional to the alkali concentration [20], which resulted in a more porous surface and spongy appearance in $SH_{8:4}$, as shown in Figure 4.

3.7. Mechanical Test. The mechanical properties of PAM and BC/PAM hydrogels (DH and $SH_{6:4}$) were measured in hydrogels with a 500% swelling and equilibrium swelling ratio. Due to the highly fragile nature of $SH_{8:4}$, it was not used to study the mechanical strength of these hydrogels. When these hydrogels (at 500% swelling) were subjected to a compressive force, they were nonbreakable, although some fractures were

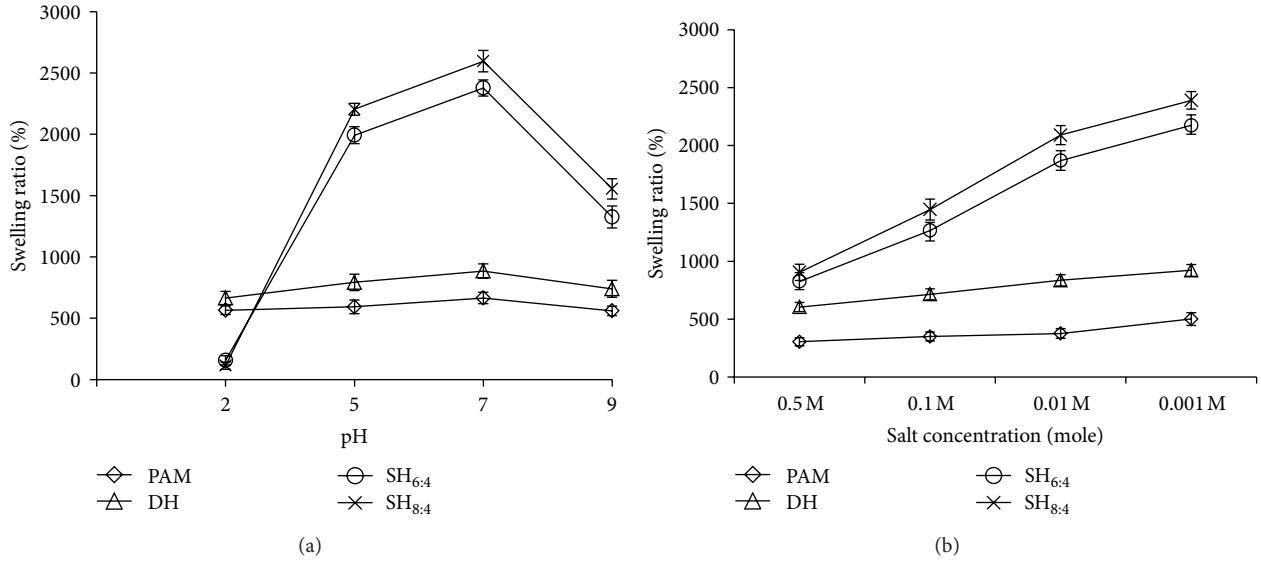

Figure 5: Swelling behavior of hydrogels at different (a) pH and (b) ionic strength.

Table 2: Mechanical properties of hydrogels ($n = 3$).

Formulation	Compressive stress (MPa) (mean ± SD)	Compressive strain (mm/mm) (mean ± SD)	Compressive modulus (MPa) (mean ± SD)
PAM[a]	0.434 ± 0.038	1.685 ± 0.083	1.592 ± 0.069
DH[a]	0.265 ± 0.025	1.961 ± 0.012	1.449 ± 0.079
$SH_{6:4}$[a]	0.410 ± 0.053	1.359 ± 0.074	1.172 ± 0.056
PAM[b]	0.562 ± 0.067	1.608 ± 0.087	1.237 ± 0.082
DH[b]	0.407 ± 0.031	1.464 ± 0.013	0.722 ± 0.026
$SH_{6:4}$[b]	0.304 ± 0.029	1.636 ± 0.093	0.229 ± 0.014

[a]Compression test of hydrogel with 500% swelling ratio.
[b]Compression test of hydrogel with equilibrium swelling ratio.

observed on the surface of the hydrogels. Conversely, when compressive force was applied on the hydrogels at equilibrium swelling, greater fracturing was observed in PAM and DH, while $SH_{6:4}$ hydrogels were completely crushed due to the lack of efficient energy dissipation and irregular distribution of cross-linking points. The Young's modulus values were 1.592, 1.449, and 1.172 for PAM, DH, and $SH_{6:4}$ hydrogels, respectively, as shown in Table 2. At 500% swelling, the Young's modulus values for PAM and DH hydrogels were comparable, but, at swelling equilibrium, it increased in the order of $SH_{6:4}$ < DH < PAM, as shown in Table 2. These data revealed that the PAM hydrogel was comparatively more elastic (less rigid) compared to the bicomponent (BC/PAM) hydrogels. XRD data also supported this finding where the bicomponent (BC/PAM) hydrogels were more crystalline (rigid) than polyacrylamide. Comparing the mechanical strength at 500% and equilibrium swelling of the hydrogels revealed that hydrogels with a higher water content showed lower mechanical strength because of the reduction in polymeric content per unit volume corresponding to an increase in swelling. The Young's modulus values of DH and $SH_{6:4}$ also indicated that grafting of nonionic PAM with BC resulted in a greater mechanical strength than that of anionic PAM. This could be due to a variation in cross-linking density in nonionic and anionic polymers.

3.8. Swelling Studies

3.8.1. pH Response. The hydrogels were allowed to swell in 50 mL of swelling media at different pHs, and the percentage swelling ratio (% SR) at 24 h is shown in Figure 5(a). The hydrogels exhibited the highest % SR at pH 7 (Figure 5(a)). The % SR of the $SH_{6:4}$ and $SH_{8:4}$ hydrogels at pH 7 (2377.47 ± 65.92 and 2595.62 ± 85.36, resp.) was approximately 2.7–3.0 times higher than the DH hydrogels (884.67 ± 45.18) and 3.6–4.0 times higher than the PAM hydrogels (664.5 ± 34.46). The percentage of swelling of the hydrogel was mainly governed by the polarity of the formulations, which was dependent on the nature of the polymers, the concentration of the cross-linking agent, and the reaction conditions. In this study, the composition of the hydrogels and the reaction conditions remained constant, and thus the degree of swelling was mainly controlled by the nature of the polymers and the solvent ratio for the dissolution of the BC. Previous studies suggested that the swelling of raw BC (cubes) is nearly irreversible after drying or compression, but it can be made repeatedly swollen by grafting with AM [9, 15, 26]. The swelling percentage of DH, $SH_{6:4}$ and $SH_{8:4}$ clearly underlie the effect of the solubility and solvent concentration on the swelling of BC hydrogels. Jin et al. reported that this solvent system has the capability of breaking hydrogen bonds, preventing the reassociation of cellulose macromolecules, and changing the highly crystalline form of cellulose into an amorphous form, resulting in remarkable changes in the swelling of the hydrogels [31]. This high pH, which is responsible for swelling, is mainly attributed to the hydrolysis of

the $-CONH_2$ group of the PAM to the –COONa group in the presence of NaOH. Electrostatic repulsion between $-COO^-$ ions creates more spaces within the hydrogel matrix, which imbibes a large amount of water [32].

The % SR was observed at different pH values to study the pH sensitivity of the hydrogels. The swelling of the hydrogels increased with increasing pH (from 2 to 7), but decreased at pH 9 as shown in Figure 5(a). The order of the pH sensitivity of the hydrogels was $SH_{8:4}$ > $SH_{6:4}$ > DH > PAM, independent of sensitivity that is specific to acidic or basic pH. The sharp change in swelling in SH was most likely due to the protonation and deprotonation of the $-COO^-$ group resulting from the partial hydrolysis of PAM at a lower and higher pH [33]. In contrast, the PAM and DH both contained nonionic PAMs, which one unable to ionize in an aqueous solution, but would undergo hydrolysis in acidic and basic solutions to produce the protonated amino ($-NH_3^+$) and carboxylic acids (COO^-) groups.

3.8.2. Ionic Strength Response. The swelling behavior of the hydrogels at different NaCl concentrations is presented in Figure 5(b). As evident from the graph, the ionic strength was inversely proportional to the % SR. This may be attributed to a change in osmotic pressure and a reduction in the repulsive forces at a higher ionic strength. The difference in osmotic pressure between water and the hydrogel was greater than the osmotic pressure difference between the salt solution and hydrogel. Thus, the swelling of the hydrogel in water was much higher than that in an ionic solution. The presence of salt reduces the osmotic pressure difference of the salt solution [20]. The lower swelling at a higher ionic strength could also be explained due to the neutralization of the carboxylate anions in the presence of Na^+, resulting in decreased electrostatic repulsive forces, which was a controlling factor for swelling [14].

3.9. Drug Release Studies. The DL% of PAM, DH, $SH_{6:4}$, and $SH_{8:4}$ was 33.78% ± 2.85%, 41.32% ± 1.95%, 58.46% ± 3.35%, and 74.56% ± 3.21%, respectively. This indicates that drug loading is dependent on the porosity and swelling properties of the hydrogels. Similarly, the *in vitro* release profile of the formulations primarily is dependent on the interactions of the drug with the polymeric network, solubility of the drug, and swelling of the hydrogel in the dissolution media. As shown in Figure 6, SH showed a higher cumulative percentage release in phosphate buffer (pH 7.4) for 8 h than that shown by DH and PAM. A similar pattern was observed in the total cumulative release, which was attributed to the swelling behavior of the hydrogels. Comparison of $SH_{6:4}$ and $SH_{8:4}$ revealed that $SH_{6:4}$ showed a lower release, which was attributed to the higher swelling and porosity in $SH_{8:4}$. The release pattern of all of the hydrogels was biphasic: first, because of the burst release due to the presence of the drug on the surface of the hydrogels, which was followed by a sustained release. An initial rapid release may be caused by the higher concentration gradient that acts as the driving force for the drug release, followed by a reduction in the release rate, which may be due to the thickness of the hydrogel acting as a diffusion barrier.

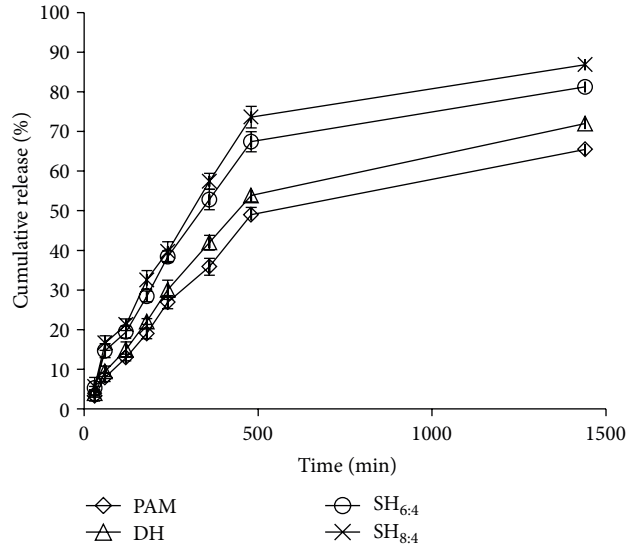

Figure 6: *In vitro* drug release profile of hydrogels in buffer pH 7.4.

The release data of the hydrogels in PBS (pH 7.4) were best fitted to zero-order release kinetics, as shown in Table 1. In addition, the release exponent of Korsmeyer-Peppas (n) of all of the formulations was in the range of 0.45–0.89, which indicated non-Fickian diffusion. The value of n indicated concurrent absorption of the dissolution media and release of the model drug, which resulted in drug release.

4. Conclusions

In this study, the accelerated microwave irradiation method was successfully used to synthesize hydrogels from BC dispersion and BC solution in a NaOH/urea aqueous system with PAM by using MBA as a cross-linker. These results suggested that the hydrogel containing cellulose in an NaOH/urea solution showed more uniform porosity structure distribution, the highest swelling property, and a higher sensitivity towards pH and ionic solution compared to that of DH and PAM. These drug release experiments revealed that SH hydrogels exhibited a higher drug loading capacity and higher drug release. From these results, it can be concluded that the SHs exhibited superior properties for drug delivery application. The pH sensitivity and superabsorbent response suggested that these smart hydrogels could be further explored for controlled oral delivery of protein, peptides, and acid-labile drugs. However, further studies are warranted to overcome the fragility and improve the mechanical properties of these hydrogels.

Acknowledgments

The authors would like to thank the Ministry of Higher Education (MOHE) and the Ministry of Agriculture (MoA), Malaysia, for their support. This project was funded by MoA: Science fund 05-01-02-SF1023 and UKM-Farmasi-02-FRGS0192-2010.

References

[1] A. G. Abadi, M. C. I. M. Amin, N. Ahmad, H. Katas, and J. A. Jamal, "Bacterial cellulose film coating as drug delivery system: physicochemical, thermal and drug release properties," *Sains Malaysiana*, vol. 41, no. 5, pp. 561–568, 2012.

[2] C. L. McCormick, P. A. Callais, and B. H. Hutchinson Jr., "Solution studies of cellulose in lithium chloride and *N*,*N*-dimethylacetamide," *Macromolecules*, vol. 18, no. 12, pp. 2394–2401, 1985.

[3] D. Klemm, B. Heublein, H. P. Fink, and A. Bohn, "Cellulose: fascinating biopolymer and sustainable raw material," *Angewandte Chemie—International Edition*, vol. 44, no. 22, pp. 3358–3393, 2005.

[4] M. Egal, T. Budtova, and P. Navard, "Structure of aqueous solutions of microcrystalline cellulose/sodium hydroxide below 0°C and the limit of cellulose dissolution," *Biomacromolecules*, vol. 8, no. 7, pp. 2282–2287, 2007.

[5] J. Cai and L. Zhang, "Rapid dissolution of cellulose in LiOH/urea and NaOH/urea aqueous solutions," *Macromolecular Bioscience*, vol. 5, no. 6, pp. 539–548, 2005.

[6] R. Jonas and L. F. Farah, "Production and application of microbial cellulose," *Polymer Degradation and Stability*, vol. 59, no. 1–3, pp. 101–106, 1998.

[7] K. Watanabe, M. Tabuchi, Y. Morinaga, and F. Yoshinaga, "Structural features and properties of bacterial cellulose produced in agitated culture," *Cellulose*, vol. 5, no. 3, pp. 187–200, 1998.

[8] S. Zhang, F. X. Li, J. Yu, and Y. L. Hsieh, "Dissolution behaviour and solubility of cellulose in NaOH complex solution," *Carbohydrate Polymers*, vol. 81, no. 3, pp. 668–674, 2010.

[9] A. Nakayama, A. Kakugo, J. P. Gong et al., "High mechanical strength double-network hydrogel with bacterial cellulose," *Advanced Functional Materials*, vol. 14, no. 11, pp. 1124–1128, 2004.

[10] J. Kim, Z. Cai, H. S. Lee, G. S. Choi, D. H. Lee, and C. Jo, "Preparation and characterization of a bacterial cellulose/chitosan composite for potential biomedical application," *Journal of Polymer Research*, vol. 18, no. 4, pp. 739–744, 2011.

[11] A. L. Buyanov, I. V. Gofman, L. G. Revel'skaya, A. K. Khripunov, and A. A. Tkachenko, "Anisotropic swelling and mechanical behavior of composite bacterial cellulose-poly(acrylamide or acrylamide-sodium acrylate) hydrogels," *Journal of the Mechanical Behavior of Biomedical Materials*, vol. 3, no. 1, pp. 102–111, 2010.

[12] N. Halib, M. C. I. M. Amin, I. Ahmad, Z. M. Hashim, and N. Jamal, "Swelling of bacterial cellulose-acrylic acid hydrogels: sensitivity towards external stimuli," *Sains Malaysiana*, vol. 38, no. 5, pp. 785–791, 2009.

[13] M. C. I. M. Amin, N. Halib, N. Ahmad, and I. Ahmad, "Synthesis and characterization of thermo- and pH-responsive bacterial cellulose/acrylic acid hydrogels for drug delivery," *Carbohydrate Polymers*, vol. 88, no. 2, pp. 465–473, 2012.

[14] N. Halib, M. C. I. M. Amin, and I. Ahmad, "Unique stimuli responsive characteristics of electron beam synthesized bacterial cellulose/acrylic acid composite," *Journal of Applied Polymer Science*, vol. 116, no. 5, pp. 2920–2929, 2010.

[15] J. Zhang, J. Rong, W. Li, Z. Lin, and X. Zhang, "Preparation and characterization of bacterial cellulose/polyacrylamide hydrogel," *Acta Polymerica Sinica*, no. 6, pp. 602–607, 2011.

[16] Z. Zhao, Z. Li, Q. Xia, H. Xi, and Y. Lin, "Fast synthesis of temperature-sensitive PNIPAAm hydrogels by microwave irradiation," *European Polymer Journal*, vol. 44, no. 4, pp. 1217–1224, 2008.

[17] J. Jovanovic and B. Adnadjevic, "Influence of microwave heating on the kinetic of acrylic acid polymerization and crosslinking," *Journal of Applied Polymer Science*, vol. 116, no. 1, pp. 55–63, 2010.

[18] Z. X. Zhao, Z. Li, Q. B. Xia, E. Bajalis, H. X. Xi, and Y. S. Lin, "Swelling/deswelling kinetics of PNIPAAm hydrogels synthesized by microwave irradiation," *Chemical Engineering Journal*, vol. 142, no. 3, pp. 263–270, 2008.

[19] A. Kumar, K. Singh, and M. Ahuja, "Xanthan-g-poly(acrylamide): microwave-assisted synthesis, characterization and in vitro release behavior," *Carbohydrate Polymers*, vol. 76, no. 2, pp. 261–267, 2009.

[20] G. B. Marandi, K. Esfandiari, F. Biranvand, M. Babapour, S. Sadeh, and G. R. Mahdavinia, "PH sensitivity and swelling behavior of partially hydrolyzed formaldehyde-crosslinked poly(acrylamide) superabsorbent hydrogels," *Journal of Applied Polymer Science*, vol. 109, no. 2, pp. 1083–1092, 2008.

[21] A. Mohanan, B. Vishalakshi, and S. Ganesh, "Swelling and diffusion characteristics of stimuli-responsive N-isopropylacrylamide and κ-carrageenan semi-IPN hydrogels," *International Journal of Polymeric Materials*, vol. 60, no. 10, pp. 787–798, 2011.

[22] Z. Peng and F. Chen, "Synthesis and properties of lignin-based polyurethane hydrogels," *International Journal of Polymeric Materials*, vol. 60, no. 9, pp. 674–683, 2011.

[23] Y. M. Mohan, P. S. K. Murthy, H. Sudhakar, B. V. K. Naidu, K. M. Raju, and M. P. Raju, "Swelling and diffusion properties of poly(acrylamide-co-maleic acid) hydrogels: a study with different crosslinking agents," *International Journal of Polymeric Materials*, vol. 55, no. 11, pp. 867–892, 2006.

[24] C. Chang, L. Zhang, J. Zhou, L. Zhang, and J. F. Kennedy, "Structure and properties of hydrogels prepared from cellulose in NaOH/urea aqueous solutions," *Carbohydrate Polymers*, vol. 82, no. 1, pp. 122–127, 2010.

[25] M. Pandey and M. C. I. M. Amin, "Accelerated preparation of novel bacterial cellulose/acrylamide-based hydrogel by microwave irradiation," *International Journal of Polymeric Materials*, vol. 62, no. 7, pp. 402–405, 2013.

[26] Y. Hagiwara, A. Putra, A. Kakugo, H. Furukawa, and J. P. Gong, "Ligament-like tough double-network hydrogel based on bacterial cellulose," *Cellulose*, vol. 17, no. 1, pp. 93–101, 2010.

[27] P. L. Ritger and N. A. Peppas, "A simple equation for description of solute release II. Fickian and anomalous release from swellable devices," *Journal of Controlled Release*, vol. 5, no. 1, pp. 37–42, 1987.

[28] C. Özeroglu and A. Birdal, "Swelling properties of acrylamide-N,N′-methylene bis(acrylamide) hydrogels synthesized by using meso-2,3-dimercaptosuccinic acid-cerium(IV) redox couple," *Express Polymer Letters*, vol. 3, no. 3, pp. 168–176, 2009.

[29] Y. Song, J. Zhou, L. Zhang, and X. Wu, "Homogenous modification of cellulose with acrylamide in NaOH/urea aqueous solutions," *Carbohydrate Polymers*, vol. 73, no. 1, pp. 18–25, 2008.

[30] S. Ouajai and R. A. Shanks, "Composition, structure and thermal degradation of hemp cellulose after chemical treatments," *Polymer Degradation and Stability*, vol. 89, no. 2, pp. 327–335, 2005.

[31] H. Jin, C. Zha, and L. Gu, "Direct dissolution of cellulose in NaOH/thiourea/urea aqueous solution," *Carbohydrate Research*, vol. 342, no. 6, pp. 851–858, 2007.

[32] S. Kim, G. Iyer, A. Nadarajah, J. M. Frantz, and A. L. Spongberg, "Polyacrylamide hydrogel properties for horticultural applications," *International Journal of Polymer Analysis and Characterization*, vol. 15, no. 5, pp. 307–318, 2010.

[33] R. da Silva and M. G. de Oliveira, "Effect of the cross-linking degree on the morphology of poly(NIPAAm-co-AAc) hydrogels," *Polymer*, vol. 48, no. 14, pp. 4114–4122, 2007.